THEORETICAL AND REVIEW ARTICLES

An information-processing model of the BOLD response in symbol manipulation tasks

JOHN R. ANDERSON, YULIN QIN, and MYEONG-HO SOHN
Carnegie Mellon University, Pittsburgh, Pennsylvania

V. ANDREW STENGER
University of Pittsburgh Medical School, Pittsburgh, Pennsylvania

and

CAMERON S. CARTER
University of Pittsburgh, Pittsburgh, Pennsylvania

Two imaging experiments were performed—one involving an algebraic transformation task studied by Anderson, Reder, and Lebiere (1996) and the other an abstraction symbol manipulation task studied by Blessing and Anderson (1996). ACT–R models exist that predict the latency patterns in these tasks. These models require activity in an imaginal buffer to represent changes to the problem representation, in a retrieval buffer to hold information from declarative memory, and in a manual buffer to hold information about motor behavior. A general theory is described about how to map activity in these buffers onto the fMRI blood oxygen level dependent (BOLD) response. This theory claims that the BOLD response is integrated over the duration that a buffer is active and can be used to predict the observed BOLD function. Activity in the imaginal buffer is shown to predict the BOLD response in a left posterior parietal region; activity in the retrieval buffer is shown to predict the BOLD response in a left prefrontal region; and activity in the manual buffer is shown to predict activity in a motor region. More generally, this article shows how to map a large class of information-processing theories (not just ACT–R) onto the BOLD response and provides a precise interpretation of the cognitive significance of the BOLD response.

Cognitive models have been increasingly successful at accounting for complex data sets on problem solving (Anderson & Lebiere, 1998; Meyer & Kieras, 1997a, 1997b; Pew & Mavor, 1998). Largely, these cognitive models have focused on latency and accuracy and, usually, only final times and accuracies. These models often specify rather complex sequences of unseen processes taking place over many seconds. Even when the pattern of data they fit is correspondingly complex, one is naturally wary of a chain of inferences about unseen processes. It would be better to have data about these intervening processes. Basically, a greater amount of converging data would be better. This article will demonstrate the potential of functional magnetic resonance imaging (f MRI) data to provide one source of converging evidence. Symmetrically, the article will show the potential of cognitive models to give a precise account of the significance of the blood oxygen level dependent (BOLD) response.

The ACT–R theory (Anderson & Lebiere, 1998), particularly in its current 5.0 version, has made itself open to such data. Figure 1 illustrates the basic architecture of that system. The external world and the internal system interact through a set of cortical buffers that hold information. Particularly important to this article are the goal buffer, the imaginal buffer, the motor buffer, and the retrieval buffer. The goal buffer keeps track of one's internal intentions in solving a problem. The imaginal buffer essentially keeps a visual image of the problem state; all problem state representations need not be visual, but they are in the algebraic tasks that we will be investigating. The manual buffer (Byrne & Anderson, 1998) is used to program hand movements and is based on the EPIC (Meyer & Kieras, 1997a, 1997b) manual processor. The retrieval buffer requests information from declarative memory and holds the retrieval results. The ACT–R 5.0 specifies when these buffers will be active during the performance of such a task and for how long.

Our main concern in this article is with the activity of these buffers in ACT–R and their corresponding cortical correlates, but we will say a little about how we assume they interact with the rest of the system shown in Figure 1. These cortical areas project to the striatum, which
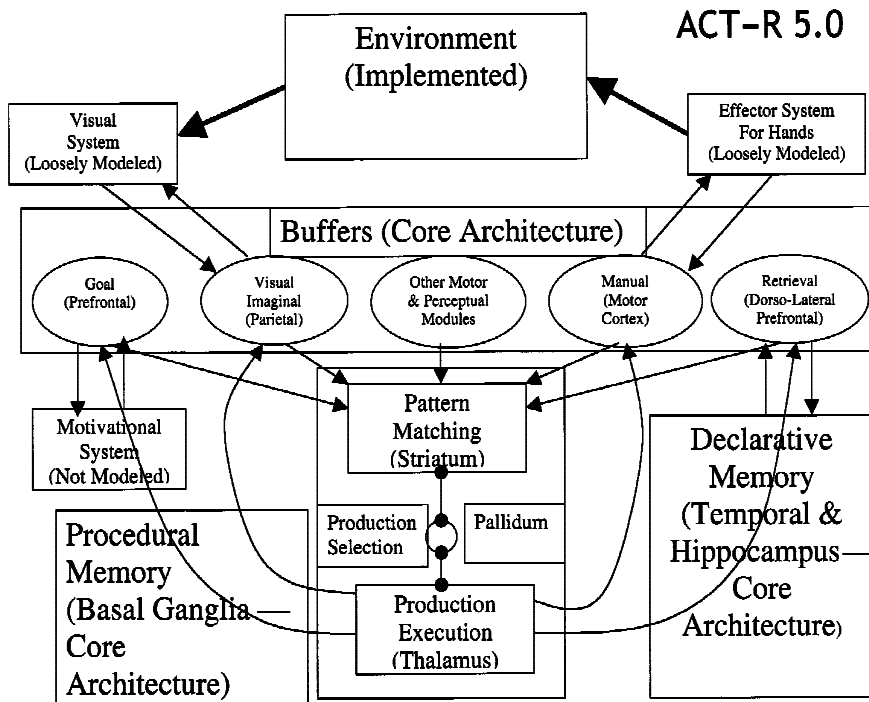
Figure 1. A representation of the information flow in ACT–R 5.0.

we hypothesize performs a pattern recognition function (in line with other proposals; e.g., Amos, 2000; Frank, Loughry, & O'Reilly, 2000; Houk & Wise, 1995; Wise, Murray, & Gerfen, 1996). The basal ganglia more generally are hypothesized to implement production rules in ACT–R, which recognize and act on patterns of activity in the cortical areas. Since production rules represent ACT–R's procedural memory, this also corresponds to proposals that the basal ganglia subserve procedural learning (Ashby & Waldron, 2000; Hikosaka et al., 1999; Saint-Cyr, Taylor, & Lang, 1988). An important function of the production rules is to update the buffers in the ACT–R architecture. The well-characterized organization of the brain into segregated cortico-striatal-thalamic loops is consistent with this hypothesized functional specialization. Thus, the critical cycle in ACT–R is one in which the buffers hold representations determined by the external world and internal modules, patterns in these buffers are recognized and a production fires, and the buffers are then updated for another cycle.

The plan of this article will be to take tasks for which there already exist well-specified ACT–R models, determine the predictions about buffer activities, and look for neural correlates. We will describe two experiments based on the research of Anderson, Reder, and Lebiere (1996) and Blessing and Anderson (1996), which were modeled in older versions of ACT–R. Anderson et al.'s paper looked at the solving of algebraic equations of different complexity, with or without a concurrent memory load. The processes we will propose for their solution do

not require any mathematics-specific faculties but require general faculties, such as those for goal maintenance, visual representation of problem state, motor programming, and declarative retrieval. To confirm that the neural correlates found in the first experiment are not specific to mathematical problem solving, we looked at the symbol manipulation task of Blessing and Anderson that removed all of the arithmetic content from algebra. This pairing of two tasks allows a strong converging test of our theory, because we can use the regions of interest (ROIs) uncovered in the one experiment to organize the fMRI data for the other experiment.

Before describing these experiments, we would like to discuss the cortical regions that we expect to see corresponding to the buffers in Figure 1. The goal and the retrieval buffers are rather difficult to separate, both in the behavior of ACT–R and in terms of their localization. Both retrieval operations and goal-setting operations have been associated with the prefrontal cortex. The hemispheric encoding retrieval asymmetry (HERA) model (Nyberg, Cabeza, & Tulving, 1996; Tulving, Kapur, Craik, Moscovitch, & Houle, 1994) associates episodic and semantic retrieval with the right and the left prefrontal cortex, respectively. In their recent review, Cabeza and Nyberg (2000) usually found that retrieval tasks produced activation in classic prefrontal areas, such as Brodmann areas (BAs) 9, 44, 45, and 46. These same areas also tend to be active in tasks that involve goal manipulations, such as task switching (Sohn, Ursu, Anderson, Stenger, & Carter, 2000), Stroop (MacDonald, Cohen, Stenger, &

Carter, 2000), and the Wisconsin card sorting task (Berman et al., 1995; Goldberg et al., 1998). In ACT–R, goal changes often require retrieval of relevant information. Thus, the predictions for the two buffers are often correlated. We will focus on the behavior of the retrieval buffer, because its behavior is somewhat easier to quantify in ACT–R, leaving open the possibility that the effects we attribute to retrieval might also be attributed to the goal buffer. In any case, the hypothesis is that use of the retrieval buffer will be correlated with activity in the prefrontal cortex. Note that the assumption is that the retrieval buffer holds the products of the retrieval but that, in line with other proposals, the actual memories are likely to be stored in other brain structures.

The visual imagery buffer holds a representation of visual problems during the course of their solution. Given that skilled algebraic manipulation is thought to be highly visual and spatial (Awtry & Kirshner, 1994; Kirshner, 1989), we would expect to see changes in the mental state of the equation represented by changes in that buffer. The literature on spatial imagery associates that with the posterior parietal cortex (BAs 7, 39, and 40). In their review, Cabeza and Nyberg (2000) noted that these regions are active in almost every study of imagery. Reichle, Carpenter, and Just (2000) found that there was greater activation in this area when participants engaged in an imagery strategy during language processing and that this was more concentrated in the left parietal regions. Perhaps it is concentrated on the left because of its connection with symbolic processing in their task. Since algebra is likewise a meaningful symbol system, our hypothesis is that activation in the left parietal region will track changes in the imaginal buffer, which in turn will reflect changes to the equation representation.

With respect to the manual buffer, it is devoted in ACT–R to representing and monitoring hand movement, usually as part of motor programming. It would be natural to associate it with the region of the motor cortex that in fact controls the hand. Including the manual buffer provides us with an anchor point in our interpretation and model fitting, since there is good prior localization of the region that is responsible for hand movements.

EXPERIMENT 1

Table 1 illustrates the six conditions of the first experiment, which were closely modeled on Anderson et al. (1996), although some changes were made to meet the methodological demands of the magnet. The equations required zero, one, or two algebraic transforma-

tions to solve. Orthogonal to this, the equations could have two letter constants in them, and the participants would have to substitute values they had just learned for these constants. Figure 2 illustrates the basic structure of the fMRI trial. The trial began with 3 sec for study of assignments for three constants. Then an equation was exposed, which might or might not involve two of these constants, and it remained on for 7.5 sec. This was followed by a white * for 7.5 sec, to allow the hemodynamic response to settle, and this was followed by a red + for 3 sec, to alert the participant to the next upcoming trial.

Anderson et al. (1996) found that this task could be understood by tracking its retrieval requirements.[1] There are two types of retrievals, which they found weighted equally in determining accuracy and latency. One type involved arithmetic retrievals, which had two subtypes: retrieving arithmetic facts such as $6 * 3 = 18$ and retrieving information about operator inverses (e.g., $-$ is the opposite of $+$, a fact that is required to undo a plus operation). The other major type was retrieval of the assignments just made of values to constants (such as $b = 5$). Although ACT–R treats these two retrievals as being of the same kind, it was not obvious that they would be so treated by the brain. Indeed, on the basis of the HERA model, one might categorize the first type of retrieval as semantic and predict that it would occur in the left prefrontal cortex and the second as episodic and predict that it would occur in the right prefrontal cortex.

Method

Task and Procedure. Table 1 shows samples of the equations used in this experiment. The participants' task was to solve the equation (i.e., isolate the x) and key in the correct answer. The answers ranged from 6 to 9. The participants used the right index, middle, ring, and little fingers in a response glove to indicate 6 through 9, respectively.

At the beginning of a trial, a memory set of three integers was presented for 3 sec, which was replaced by an algebra equation. The participants were instructed to rehearse these integers until the equation appeared. Half of the algebra equations required substitution of constants with these integers, but the participants had no warning of which equations would use constants. No additional tasks were required regarding the memory set, other than the substitution. The equation itself remained on the screen for 7.5 sec. If no response was given during this time, the trial was scored as incorrect. The equation then was replaced by an asterisk (*) for 7.5 sec of rest. Finally, a plus sign (+) appeared for 3 sec of warning for the next trial.

Parametric design. Two factors were manipulated. First, the equations differed in computational complexity. The zero-transformation problems did not require any algebraic transformations. These equations always contained 1 as the slope and 0 as the intercept (e.g., $1x + 0 = 06$). Therefore, the answer would be the integer on the

Table 1
Example of the Materials in the Algebra Experiment Extension of
Anderson, Reder, and Lebiere (1996)

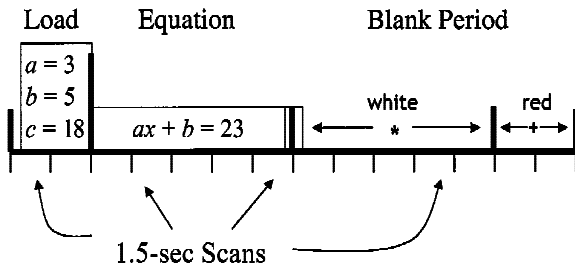| Transformations	No Substitution	Substitution
0	$1x + 0 = 06$	$ax + 0 = c$ ($a = 1$; $c = 6$)
1	$2x + 0 = 12$ or $1x + 9 = 18$	$ax + 0 = c$ ($a = 2$; $c = 12$)
2	$3x + 5 = 23$	$ax + b = 23$ ($a = 3$; $b = 5$)

Figure 2. The 21-sec structure of an fMRI trial in Experiment 1.

right-hand side of the equation. The one-transformation problems required removing either the intercept or the slope from the left-hand side of the equation, but not both. Solving the two-transformation problems required removing both the intercept and the slope. The rather unusual presentation format of algebra equations that we adopted (such as representing 1 and 0 in the simpler problems) was to keep the visual fields of the stimuli as constant as possible across different problem complexities.

Second, the integers for an equation either were directly available from the equation (no substitution) or had to be retrieved from the memory set (substitution). The memory set consisted of three integers. The participants were instructed to treat them as the values for the constants a, b, and c, in left-to-right order. In the substitution condition, the subsequent equation contained two of these constant letters (e.g., $a x - b = 12$), and a participant had to retrieve the values for these constants to solve the equation.

Prescan practice. The participants took about 30 min of prescan practice on the day before the scan. At first, a key practice program was run to acquaint them with the finger-to-key mapping with a hand-held response glove (press the index finger for 6, the middle finger for 7, the ring finger for 8, and the little finger for 9). Then there were four blocks of task practice, 18 trials for each block. The feedback on accuracy and latency was given at the end of each trial in the first two blocks. In the last two blocks, no trial-by-trial feedback was given to correspond to the procedure in the scanner.

Event-related fMRI scan. Event-related fMRI data were collected by using a single-shot spiral acquisition on a GE 3T scanner, 1,500-msec TR, 18-msec TE, 70° flip angle, 20-cm FOV, 28 axial slices/scan with a 3.2-mm-thick 64×64 matrix, and with AC–PC on the 8th slice from the bottom. There were 14 scans (21 sec) for each trial, 18 trials for a block, and eight blocks for each participant. There was no trial-by-trial feedback. The protocol of each trial of scan is illustrated in Figure 2.

Images acquired were analyzed using the NIS system.[2] Images first were realigned using 12-parameters AIR (Woods, Grafton, Holmes, Cherry, & Mazziotta, 1998) and then cross-registered to a common reference brain by minimizing signal intensity difference, after which functional images were set to a standard mean intensity, smoothed (8-mm FWHM 3-D Gaussian kernel) and pooled across participants to improve signal-to-noise ratio. Spatial F maps were generated using an analysis of variance (ANOVA). ROIs were identified by thresholding spatial F maps of condition (with the requirement of six contiguous voxels, $p \leq .01$, with degrees of freedom corrected by Greenhouse–Geisser).

Participants. The participants were 8 right-handed native English speakers (4 females). Their ages ranged from 19 to 23 years, with an average of 21.5.

Results

Average accuracy was 84.7%, and accuracy showed a strong negative correlation with latency ($r = -.878$). Only correct trials were analyzed. Figure 3 shows the latency results from the experiment. There were large and significant effects of both number of transformations [$F(2,14) = 260.44, MS_e = 81,806, p < .0001$] and substitution [$F(1,7) = 135.14, MS_e = 154,207, p < .0001$] and no interaction between these factors [$F(2,14) = 0.83, MS_e = 74,115$]. As can be seen, these latency effects are consistent with the ACT–R model that we will present.

Analysis of fMRI data was also restricted to trials on which the participants were accurate. ROIs were selected according to the interaction term in a 6 conditions $\times$ 14 scans ANOVA. To have a conservative test that dealt
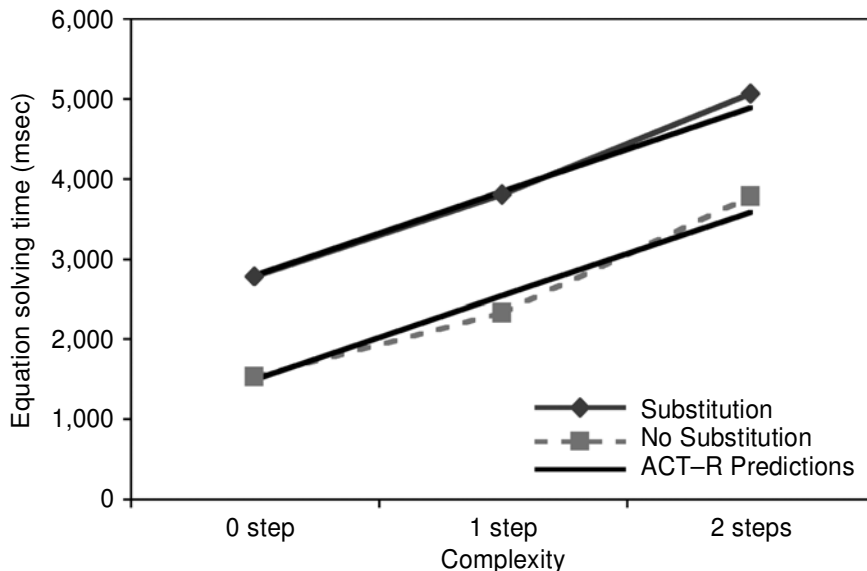

Figure 3. Mean latency in Experiment 1 as a function of number of transformations for the substitution and the no-substitution conditions.

with nonindependence of successive scans, we used the correction of assigning only five degrees of freedom to the numerator in the F statistic for the interaction term (the Greenhouse–Geisser correction for nonindependence of conditions). The interaction was examined in each voxel, and the selected regions met the criteria of a minimum of six contiguous voxels with a significant interaction at $p \le .01$ (Forman et al., 1995). Figure 4 and Table 2 give the seven regions that achieved this level of significance. Figure 4 displays only the top 16 slices, since no significant ROIs were found lower in the brain. ROI 1 is the intraparietal sulcus, which has been found to be active in almost all studies of mathematical thinking (e.g., Dehaene, Spelke, Pinel, Stanescu, & Tsivkin, 1999; Gruber, Indefrey, Steinmetz, & Kleinschmidt, 2000; Menon, Rivera, White, Glover, & Reiss, 2000; Rickard et al., 2000; Zago et al., 2001). ROI 2 is the anterior cingulate gyrus. ROI 3 is the precuneus, which has also been found to be active in a number of studies of mathematical thinking (e.g., Dehaene et al., 1999; Zago et al.,

2001). ROI 4 is the left inferior frontal gyrus (BA 44), which again has been found to be active in almost all studies of mathematical thinking. ROI 5 is a prefrontal region at the border between BAs 45 and 46, which has also been found to be active in some studies (Gruber et al., 2000; Zago et al., 2001). Regions 6 and 7 are the left and the right supramarginal gyrus (BA 40). Except for ROI 2, which is central, and ROI 6, which is right, the areas of activation are in the left cortex. This lateralization is typical of imaging studies of mathematical tasks. Damage in the vicinity of ROIs 1, 3, and 7 has also been shown to be associated with acalculia or dyscalculia (Grafman & Rickard, 1996; Jackson & Warrington, 1986; Rosselli & Ardila, 1989).

Figure 5 shows the activation functions for these seven regions, averaged over conditions, as a function of the 14 scans. The dependent measure is percentage of activation over the baseline set by the average of Scans 1 and 2 (before the equation) and Scans 13 and 14 (by which time the BOLD signal should return to baseline). ROIs
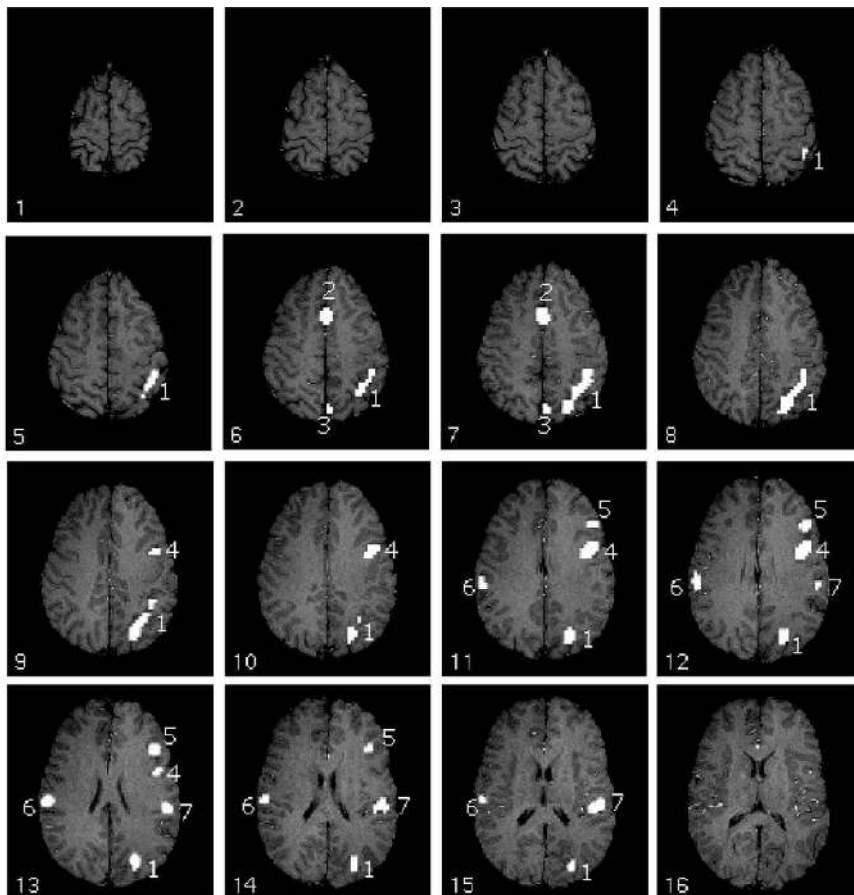

Figure 4. Activation map for the top 16 slices showing areas in Experiment 1 with a significant interaction between scan and condition. Only regions with more than six contiguous voxels and $p <$ .01 are shown. See Table 2 for identification of the regions. The AC–PC line is 5 slices below Slice 16 in this figure. This observes the radiological convention of displaying the left side of the brain on the right.

Table 2
Regions of Interest, Location of Centroids, and Significances for Experiment 1

			Stereotaxic Coordinates (mm)			F	
Region of Interest	Brodmann Area	Voxel Count	x	y	z	Maximum	Average
1. Left posterior parietal	39, 40	190	−30	−55	38	5.50	4.09
2. Anterior cingulate	32	32	1	15	39	4.56	3.98
3. Left precuneus	7	10	−2	−66	45	4.27	3.98
4. Left inferior frontal gyrus	44	62	−43	4	23	5.19	4.19
5. Left prefrontal	45/46	29	−42	28	18	4.78	4.02
6. Right supramarginal gyrus	40	33	58	−18	22	4.13	3.81
7. Left supramarginal gyrus	40	36	−51	−20	19	4.41	3.86

1–5 show relatively similar rises and falls. Table 3 shows the intercorrelations among the 84 observations (14 scans × 6 conditions) of the percentage of change obtained for each of the seven ROIs. The posterior parietal ROIs 1 and 3 are quite similar, with correlations over .9, as are the frontal ROIs 4 and 5. Although these are the highest intercorrelations, the intercorrelations are positive and fairly strong, except for those with the supramarginal ROIs 6 and 7, which do not correlate strongly with any region except each other. In Figure 5, ROIs 6 and 7 display somewhat peculiar but similar average functions, first falling below zero and then rising above zero. Rickard et al. (2000) and Zago et al. (2001) found deactivation in these regions when participants perform calculations.

We will focus our analyses on ROI 1 and ROI 5. Both ROIs 1 and 3 are from the left posterior parietal region that we would expect to be associated with the imaginal buffer in ACT–R. ROI 1 was chosen because it is larger and more reliable, but note its high correlation with ROI 3. The two frontal regions, ROI 4 and ROI 5, also

behave similarly. We have chosen to focus on ROI 5 because it is more clearly prefrontal. We also chose a third area for investigation, which did not prove to yield a significant interaction in this experiment but did in the next experiment. This is a region that covers the motor and sensory regions corresponding to the right hand. Its exact coordinates will be given as part of Experiment 2 (see ROI 1 in Table 7). These three regions of interest are illustrated in Figure 6.

Figure 7 contrasts the behavior of these three regions in the two extreme conditions—no transformation with no substitution versus two transformations with substitution. All the regions show effects of condition but show different patterns. The posterior parietal and the prefrontal particles are quite similar in the most complex condition of two transformations with substitution. However, they are dramatically different in the simplest condition of no transformations and no substitution. In this simplest condition, the posterior parietal particle shows about half the rise of that in the most complex condition, whereas the prefrontal particle appears to show no effect.
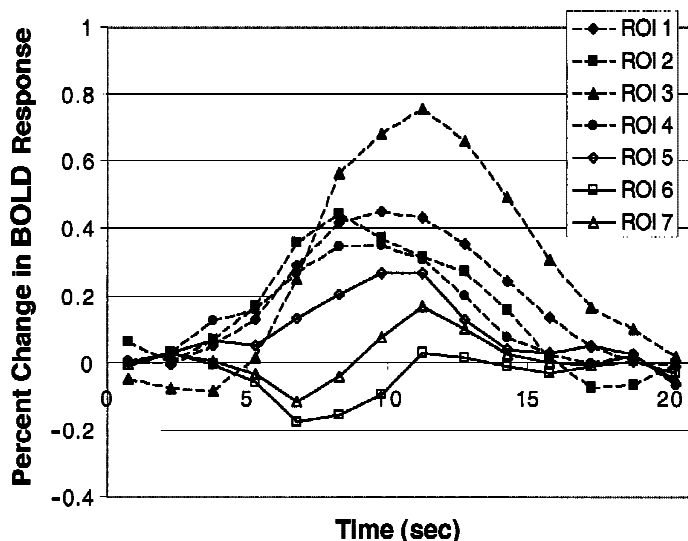

Figure 5. Average activation functions for the seven regions of interest from Experiment 1.

Table 3
Intercorrelations Among the Activation Functions in the Various Regions of Interest Identified in Experiment 1

	ROI 2	ROI 3	ROI 4	ROI 5	ROI 6	ROI 7
ROI 1	.824	.918	.814	.703	−.364	.201
ROI 2		.686	.609	.404	−.325	−.008
ROI 3			.632	.600	−.207	.304
ROI 4				.908	−.536	.0508
ROI 5					−.551	.0495
ROI 6						.699

Thus, the prefrontal particle is more sensitive to our complexity manipulations. The motor particle does not show greater magnitude of response in the more complex condition but shows a greater delay in peaking and a wider distribution, which would be consistent with the execution of a later and more variably timed response.

PREDICTING THE BOLD SIGNAL

In this section, we will first describe how to map the activity of an information-processing model onto predictions of the BOLD signal, and we will then describe the ACT–R predictions. Figure 8 illustrates the behavior of the three relevant buffers in ACT–R. Each box in that figure reflects a period of time during which that buffer (buffers correspond to columns of the figure) is active, and the vertical length of the box reflects the duration that the buffer is active. In the next section, we will discuss how one goes from charts like this to predictions of the BOLD function. In the subsequent section we will discuss the ACT–R model that produces the behavior illustrated in Figure 8.

Mapping Buffer Activity Onto the BOLD Function

Figure 9 illustrates the general idea about how we map from events in an information-processing model, such as those illustrated in Figure 8, onto the predictions of the BOLD function. Each buffer will generate a BOLD function in an associated region, and Figure 9 represents the events in one hypothetical buffer and the resulting BOLD function. In this hypothetical case, we assume that the buffer is active for 150 msec from 0.5 to 0.65 sec, for 600 msec from 1.5 sec to 2.1 sec, and for 300 msec from 2.5 to 2.8 sec. The bars at the bottom of the graph indicate when the buffer is active.

A number of researchers (e.g., Boyton, Engel, Glover, & Heeger, 1996; Cohen, 1997; Dale & Buckner, 1997) have proposed that the BOLD response to an event varies according to the following function of time, t, since the event:

$$B(t) = t^a e^{-t},$$

where estimates of the exponent have varied between 2 and 10 (and we will constrain our estimates within these bounds). This is essentially a gamma function that will reach maximum a time units after the event. As is illustrated in Figure 9, this function is slow to rise, reflecting the lag in the hemodynamic response to neural activity.

We propose that while a buffer is active, it is constantly producing a change that will result in a BOLD response according the above function. The observed fMRI response is integrated over the time that the buffer is active. Therefore, the observed BOLD response will vary with time as

$$CB(t) = M \int_0^t i(x) B\left(\frac{t-x}{s}\right) dx,$$

where M is the magnitude scale for response, s is the latency scale, and $i(x)$ is 1 if the buffer is occupied at time x and 0 otherwise. Note that because of the scaling factor, the prediction is that the BOLD function will reach maximum at roughly $t = a * s$ sec.[3] Note that the function reaches a maximum and comes down because the period of activity in the buffer is brief. If there were sustained
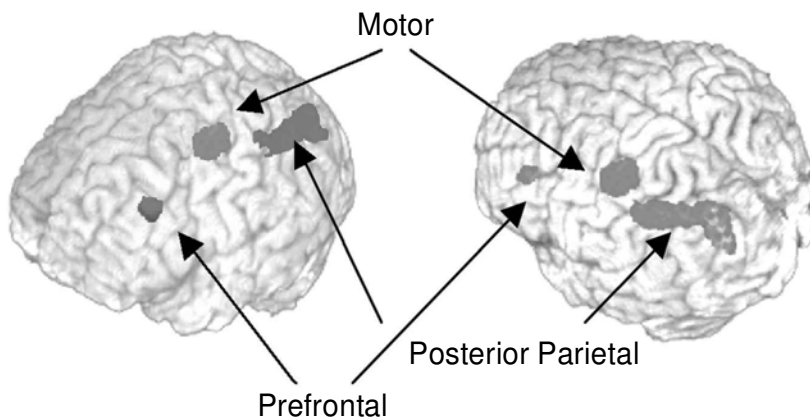

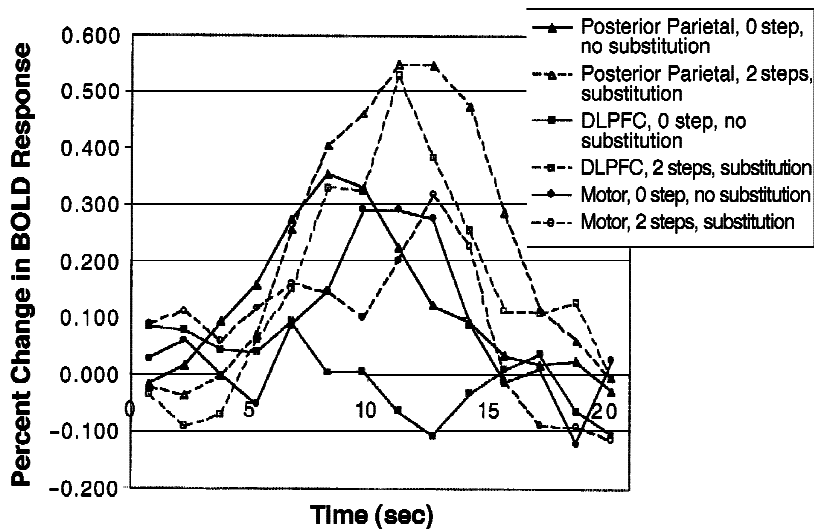Figure 6. An illustration of the three left regions of interest for modeling.

Figure 7. Contrasting behavior of the three focus regions in the two most extreme conditions of the experiment.

activity in the buffer, the BOLD response would reach a maximum level and sustain it. The prediction of the maximum at $t = a * s$ is only relatively precise when the duration of the activity is relatively brief.

As Figure 9 illustrates, one can think of the observed BOLD function in a region as reflecting the sum of separate BOLD functions for each period of time the buffer is active. Each period of activity is going to generate a BOLD function according to a gamma function, as has been illustrated. The peak of the BOLD functions reflects roughly when the buffer was active but is offset because of the lag in the hemodynamic response. The height of the BOLD function reflects the duration of the event, since the integration makes the height of the function proportional to duration over short intervals.

Note that this model does not reflect a frequent assumption in the literature (e.g., Just, Carpenter, & Varma, 1999) that a stronger BOLD signal reflects a higher rate of metabolic expenditure. Rather, the assumption is that it reflects a longer duration of metabolic expenditure. The two assumptions are relatively indistinguishable in the BOLD functions they produce, but the time assumption more naturally maps onto an information-processing model that assumes stages taking different durations of activity. Since these processes are going to take longer, they will generate higher BOLD functions, without our having to make any extra assumptions about different rates of metabolic expenditure. The total area under the curve in Figure 9 will be directly proportional to the period of time that the module is active. If a module is active for a total period of time T, the area under the BOLD function will be $M*\Gamma(a + 1) * T$, where Γ is the gamma function [in the case of integer a, note that $\Gamma(a + 1) = a!$].

Since the area under the BOLD function reflects the proportion of time the region is engaged, it is useful to try to come up with empirical estimates of the area under

the function. For the 18 conditions defined by crossing the three ROIs illustrated in Figure 6 with the 6 conditions of the experiment, we estimated the area under the BOLD function as the amount Scans 3–12 were above the baseline defined by Scans 1 and 2 (before the equation was given) and Scans 13 and 14 (by which time the BOLD function should have returned to baseline).

Figure 10 gives the resulting estimates of area under the curves for the three regions as a function of condition. As can be seen, there are three quite distinct patterns. Both the posterior parietal region and the prefrontal region show a strong effect of condition, but the difference is that the prefrontal region has effectively no area in the simplest condition, implying that the region is not at all active. In contrast, the posterior parietal region is about half as active in the simplest condition as in the most complex condition. The motor area does not seem to vary substantially with condition. [Note that the curves being measured for the extreme conditions (zero transformations, zero substitutions vs. two transformations, two substitutions) are illustrated in Figure 7.]

ACT–R Predictions

We will now describe the ACT–R model that we developed to fit the behavior profile in Figure 3 and the BOLD responses for the three selected regions. A complete ACT–R model for performing the experiment and all the conditions is available at the Published ACT–R Models link from http://act.psy.cmu.edu. It was based on the model in Anderson et al. (1996) but has been updated from ACT–R 2.0 to ACT–R 5.0. Its two essential aspects are a sequence of transformations of the internal representation of the equation and retrievals. Figure 8 illustrates these for the most complex condition of two transformations with substitution (see Table 1). Although there are other internal computations, the critical steps involve
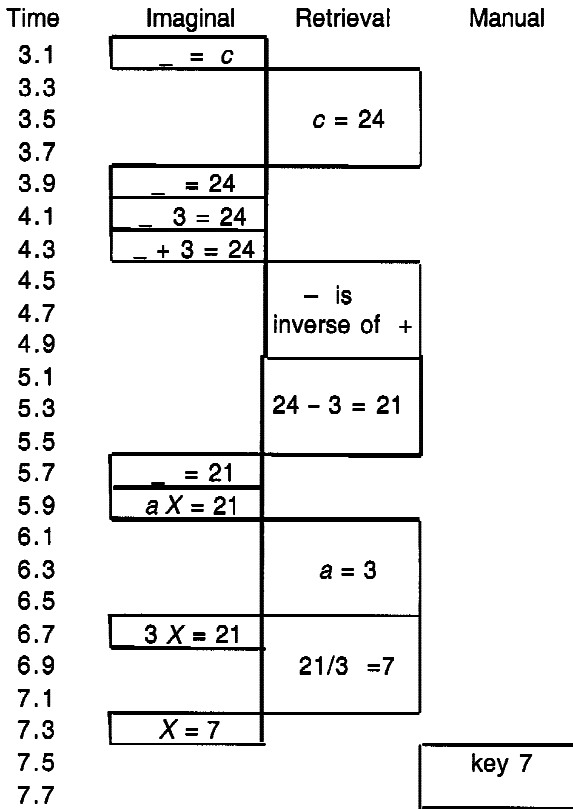
Time	Imaginal	Retrieval	Manual
3.1	_ = c		
3.3			
3.5		c = 24	
3.7			
3.9	_ = 24		
4.1	_ 3 = 24		
4.3	_ + 3 = 24		
4.5		– is	
4.7		inverse of +	
4.9			
5.1			
5.3		24 – 3 = 21	
5.5			
5.7	_ = 21		
5.9	a X = 21		
6.1			
6.3		a = 3	
6.5			
6.7	3 X = 21		
6.9		21/3 = 7	
7.1			
7.3	X = 7		
7.5			key 7
7.7			

Figure 8. The approximate time line for the buffer activity in the ACT–R model of Experiment 1. The processing is illustrated beginning 3 sec after the study of the constant assignments and with presentation of the equation (see Figure 2).

imaginal transformations, which take 200 msec each, retrieval operations, which take an estimated 600 msec, and a final motor operation, which takes 400 msec. Only the retrieval time of 600 msec was estimated to fit the behavioral data, and the other values derive from default pa-

rameters in ACT–R. ACT–R has a theory of the microstructure of these retrievals, but for present purposes, we can treat them as simply taking this fixed time.

The equations have four significant symbols that have to be encoded: the term on the right (the c in Figure 8), the first term on the left (the 3 in Figure 8), the operator (the + in Figure 8), and the term before the X (the a in Figure 8). Each time one of these symbols is encoded, there is a transformation in the visual image of the equation. The other two symbols (the X and the =) are predictable and are encoded into the equation as part of one of these transformations. In addition, the visual image is transformed if there is a substitution or an algebraic transformation. Thus, depending on condition, the number of transformations of the visual image is

$$V = 4 + 2S + A,$$

where $S = 0$ if there are no substitutions and 1 if there are and A is the number of algebraic transformations.

Two retrievals are required in the case of substitution, one for each algebraic fact retrieved and one to retrieve the inverse of the + or −. (We assume that an inverse operator need not be retrieved in the case of the second operation, because it is always *divide*.) Thus, the number of retrievals is

$$R = 2S + 1.5A,$$

where the 1.5 reflects the fact that two retrievals are required to remove the intercept but only one to remove the slope.

Finally, there is always just one motor action, and its timing varies with the timing of the response. The fact that there is just a single action may explain why the motor area did not appear as a significant region in this experiment. It will be significant in the next experiment, where five fingerpresses will be required.

Figure 11 shows the amount of time each buffer is active in each condition. This should be compared with Figure 10, which gives the area under the BOLD functions
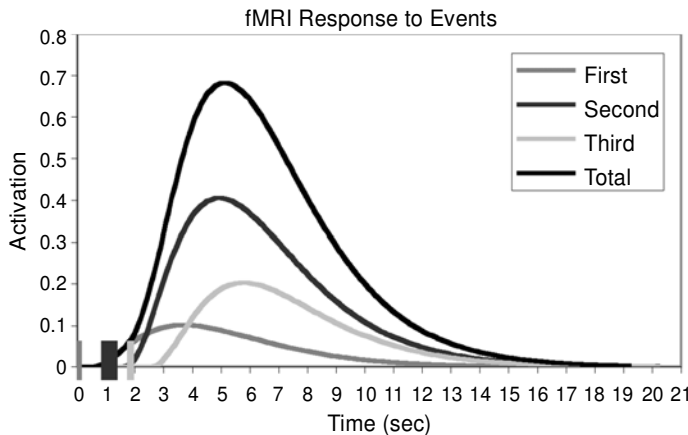

Figure 9. An illustration of how the BOLD functions from three different length events result in an overall BOLD function.
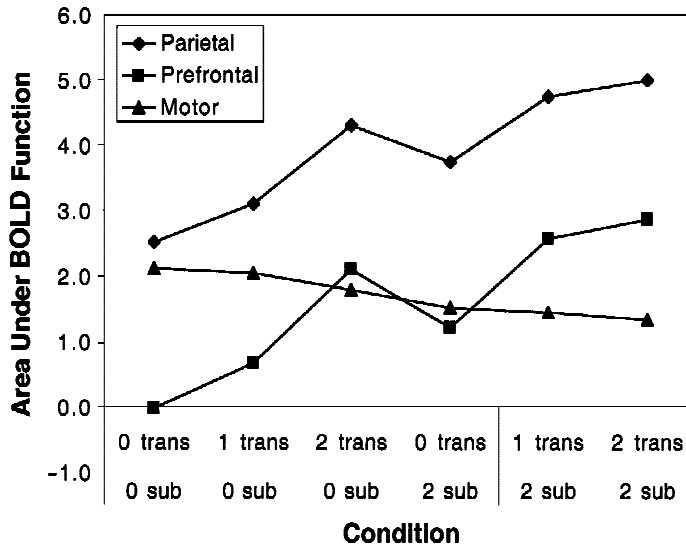
Figure 10. The area under the BOLD function for the six different conditions for each of the regions of interest. Trans, transformation; sub, substitution.

for the three regions. Recall that the area under the curve, by hypothesis, is proportional to the time the region is active. Therefore, we asked how close the time patterns (T_i) for various buffers in Figure 11 matched the areas (A_i) for various regions in Figure 10. To do this, we calculated the analogue of an R^2 measure for proportionality:

$$\text{Proportionality} = \frac{\left(\sum_i T_i A_i\right)^2}{\sum_i T_i^2 \sum_i A_i^2}.$$

Note that in the definition of the standard R^2, one replaces the raw scores in the above by the deviations from the mean. Table 4 reproduces the measures of proportionality between various regions and the time of the buffer. It clearly confirms the association of the parietal region with the imaginal buffer, the prefrontal region with the retrieval buffer, and the motor region with the manual buffer. It is worth emphasizing that, whereas the fits we will display depend on parameter estimation, this proportionality test is a parameter-free prediction depending only on the number of transformations, retrievals, or motor actions. It does not depend on the pa-
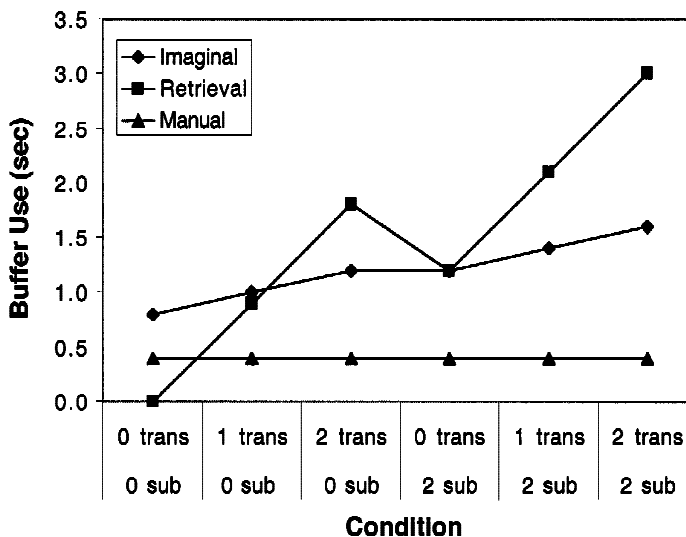

Figure 11. The total amount of time that an ACT–R buffer is in use for the six different conditions for each of the regions of interest. Trans, transformation; sub, substitution.

Table 4
Measures of Proportionality Between Buffer Activity and Area Under the BOLD Function in Experiment 1

Buffer	Parietal	Prefrontal	Motor
Imaginal	.994	.822	.852
Retrieval	.872	.951	.622
Manual	.954	.662	.917

rameters a and s that we estimate to characterize the exact size and shape of the BOLD function. It also does not depend on the estimated duration of the imaginal, retrieval, and manual operations; rather, it depends only on the number of these operations.

So far, we have produced evidence for the hypothesized association among regions and buffers. These associations are based just on the correspondence between the activity of the buffer and the area under the BOLD function. We have yet to show that the behavior of ACT–R's buffers can account for the detailed time course of the BOLD signal. Establishing the correspondence in Table 4 is a necessary but not sufficient condition for the ACT–R buffers to predict the BOLD signals.[4] We will now see whether we can fit BOLD functions to the functions for each condition in each region, assuming the hypothesized association of buffers to regions. Since there were three ROIs, six conditions, and 14 scans, this means we were fitting $3 \times 6 \times 14 = 252$ observations. To fit these data required estimating the basic parameters of the BOLD function, which are M, s, and a. We estimated separate parameters for each region because there is evidence that the exact form of the BOLD function can change from region to region (e.g., Huettel & McCarthy, 2000; Kastrup, Krüger, Glover, Neumann-Haefelin, & Moseley, 1999).

The parameters used in fitting the BOLD functions are reproduced in Table 5. These parameters were estimated by trying to minimize the following quantity:

$$\sum_{i \in \text{ROIs}} \sum_{j \in \text{Conditions}} \sum_{k \in \text{Scans}} (\overline{B}_{ijk} - \hat{B}_{ijk})^2 / s_i^2,$$

where $\overline{B}_{ijk}$ is the mean BOLD response, $\hat{B}_{ijk}$ is the predicted response, and s_i^2 is the mean error in the BOLD response for ROI i calculated by the interaction between the 84 values (6 conditions $\times$ 14 scans) and the 8 participants. Under the hypothesis that all deviations are normally distributed noise, this quantity is distributed as a chi-square with degrees of freedom equal to the number of observations (252) minus parameters (9)—that is, 243 degrees of freedom. The value of this quantity is 340.83, which is quite significant, indicating, not surprisingly, that there are things in the data not predicted by the model. On the other hand, it is not radically different from its expected value of 243 (i.e., the degrees of freedom), indicating that we are capturing most of the systematic variance.[5]

Figures 12–14 reproduce the fits of the model to the data. As can be seen, the actual quality of the fits are generally good, with correlations from .955 to .998. The

fits of the imaginal buffer activity are particularly good, probably reflecting the large size of the posterior parietal particle and, hence, accurate estimate of the means. The fits to the prefrontal particle are quite good and again capture the relative magnitude, which is a parameter-free prediction of number of retrievals. In this case, we have a confirmation of Anderson et al.'s (1996) production system model's assumptions about number of retrievals. The fits to the motor region are slightly less good, reflecting the relatively poor signal-to-noise ratio. Still, the prediction is confirmed that the peak of the BOLD response would shift with the time of the response.

Both the prefrontal particle and the motor particle show some evidence that, at the end, the BOLD response actually goes below zero and then comes back up. This is the major source of the systematic deviations in the fits of the functions. Glover (1999) has found similar behavior in the motor region, and he is able to predict this as the difference of two separately parameterized BOLD functions. We did not want to add such complications to our model for this article. At the end of the article, we will return to this and other complications that could be added to the mathematical treatment of the BOLD response.

EXPERIMENT 2

Our explanation of the BOLD functions did not depend on the mathematical content of the problems. As was noted, other researchers have associated left parietal and left prefrontal regions with arithmetic processing. The second experiment was performed to confirm that our chosen areas would show similar responses in problems without real mathematical content. This second experiment was similar to the first in that it involved symbol manipulation, but it did not involve the calculation of arithmetic facts and used characters as arbitrary symbols (although the characters were still digits, to facilitate finger mapping). This experiment also served as an independent test of the functional assignment of the three areas of interest.

The experiment was adapted from the paradigm of Blessing and Anderson (1996), who were interested in how college students would learn to perform transformations like those in algebra.[6] Our experiment did not

Table 5
Parameters of the BOLD Function Estimated for Experiments 1 and 2

Parameter	Imaginal	Retrieval	Manual
Experiment 1			
Scale (s)	1.647	0.691	0.635
Exponent (a)	3.054	8.180	7.431
Magnitude: $M\,\Gamma(a+1)$*	3.486	0.933	3.826
Experiment 2			
Scale (s)	2.158	0.543	1.687
Exponent (a)	2.559	10.000	2.732
Magnitude: $M\,\Gamma(a+1)$*	2.379	0.657	4.798

*This is a more meaningful measure, since the height of the function is determined by the exponent as well as by M.
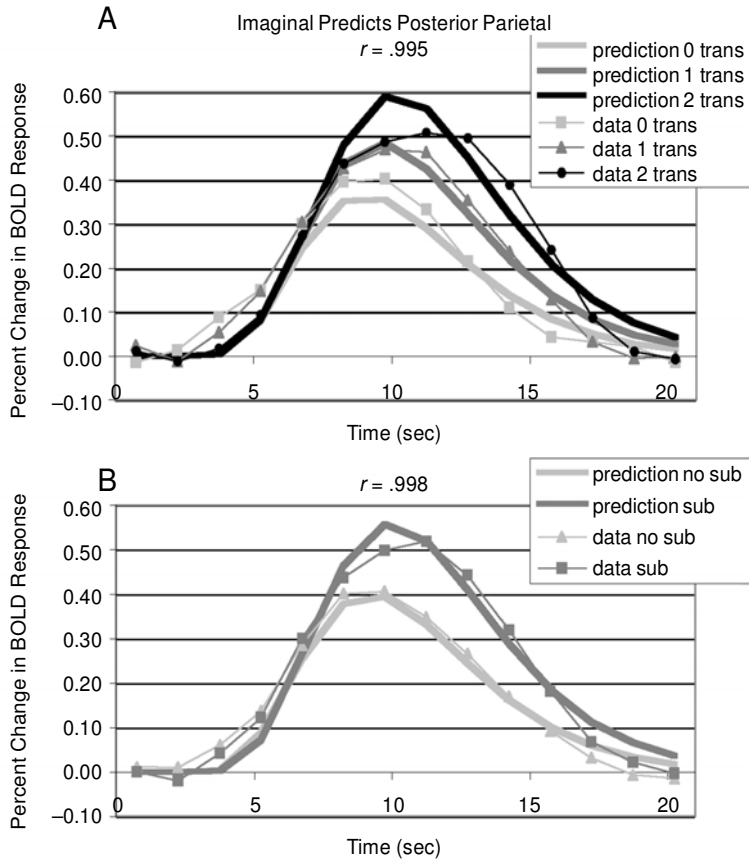
Figure 12. Ability of the imagery buffer to predict the posterior parietal particle: (A) effects of number of transformations and (B) effects of substitution.

involve as much training as that in Blessing and Anderson, and so our interest was not in learning, but only in the effect of number of transformations. Table 6 illustrates the conditions of our experiment. The participants saw strings that were divided into a left and a right side by a ↔. On both sides of this symbol was a sequence of symbols that consisted of operators and operands. Operators were encased in circles. The participants' task was to isolate the special symbol ϼ on the left and then type all of the symbols that appeared on the right. In the zero-transformation condition, the string was already in this format, and the participants simply had to type the four symbols on the right. In the one-transformation condition, there was an operator on the left before the ϼ, which had to be removed by *undoing*. There were four operators, and each had different rules for undoing: ② was undone by switching all ② operators on the right to ③ and vice versa; ③ was undone by switching the order of the two operands on the right; ④ was undone by switching all ④ operators on the right to ⑤ and vice versa; and ⑤ could be undone by simply removing it.

The participants had to memorize these four rules for undoing and apply them. In the third condition (two transformations) there were also an operator and an

operand after the ϼ, which had to be removed. There were additional rules for removing these, which involved inverting the operator and moving the inverted operator and the operand over to the right. The ② and ③ operators were inverses of each other, as were the ④ and ⑤ operators. Order of precedence required that these two symbols first be moved over to the right side before the operator before the ϼ could be undone.

In all cases, four symbols had to be typed for the answer. The participants were required to complete all transformations in their head before beginning to type the answer. When they had done so and were ready to output the answer, they pressed their thumb and then keyed the four numbers in the answer with their other fingers. The answers were always some sequence of the digits 2–5.

Table 6
Examples of the Materials in the Symbolic Reasoning Experiment Based on Blessing and Anderson (1996)

Steps	Equation	Answer
0	ϼ ↔ ③4②5	ϼ ↔ ③4②5
1	②ϼ ↔ ③4②5	ϼ ↔ ②4③5
2	②ϼ ③4 ↔ ②5	ϼ ↔ ③5③4

Retrieval Predicts Prefrontal
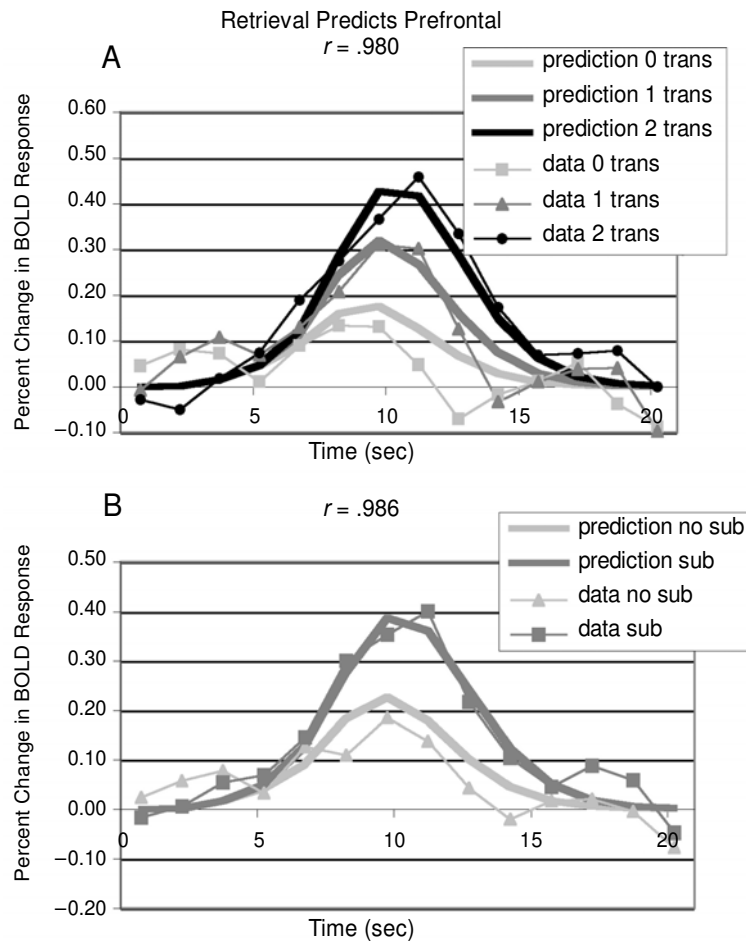
A   *r* = .980

B   *r* = .986

Figure 13. Ability of retrieval buffer to predict the prefrontal particle: (A) effects of
number of transformations and (B) effects of substitution.

They were given 1.5 sec to key each digit, to discourage efforts to compute the answers on the fly. In fact, the time to key the four digits did not vary with condition, and only the time for the thumbpress varied. The structure of the fMRI trial is illustrated in Figure 15.

Method

Only one factor, computational complexity, was manipulated in the data analysis of this experiment. The zero-step transformation problems required no symbol arrangement, but simply copying the answer. The one-step transformation problems required only elimination of the operator symbol. The two-step transformation problems required first moving terms over to the left side and then elimination.

Trial procedure. A trial began with a prompt, which was a column of two rectangles. In the first rectangle, there was an indication of the complexity of the upcoming problem. After 1.5 sec, the first rectangle was filled with the problem. The participants were instructed to solve the problem mentally and to press the thumb key when they were ready to key in the final solution, at which time the problem in the first rectangle disappeared. The thumbpress provided a measure of the planning time. If the plan time exceeded 18 sec, the trial was scored as incorrect. After the thumbpress, they had 1.5 sec to press a key for each of four symbols in the answer. The correct answer appeared on the second rectangle as the participants typed in, even when they typed in a wrong answer or missed

the 1.5-sec response window. The full answer remained on the screen for another 1.5 sec, followed by a 6-sec rest period with a visual stimulus as a column of two empty rectangles.

Prescan practice. On the day before the scan day, there was a prescan session that lasted about 45 min. The participants were introduced to the set of rules, practiced finger-to-key mappings, and practiced actual problem solving. They first practiced 12 problems from the most complex two-step transformation problems with a detailed step-by-step solution, then 24 problems of all three problem complexities with a detailed step-by-step solution, and then 12 more problems from all three complexities with no step-by-step solution.

Event-related fMRI scan. The parameters of the event-related fMRI scan were the same as those in the algebra equation solving experiment. There were 15 blocks in the functional scan, with 5 min and 30 sec for each block. We analyzed the first 12 scans, starting from the 1 scan before the presentation of the prompt.

Participants. Group analysis was done from 8 participants' data (right-handed native English speakers, 3 males/5 females, from 18 to 27 years of age, with an average of 20.6).

Results

Figure 16 shows the latency results from the experiment. There were large and significant effects of number of transformations [$F(2,14) = 153.12$, $MS_e = 256,156$,
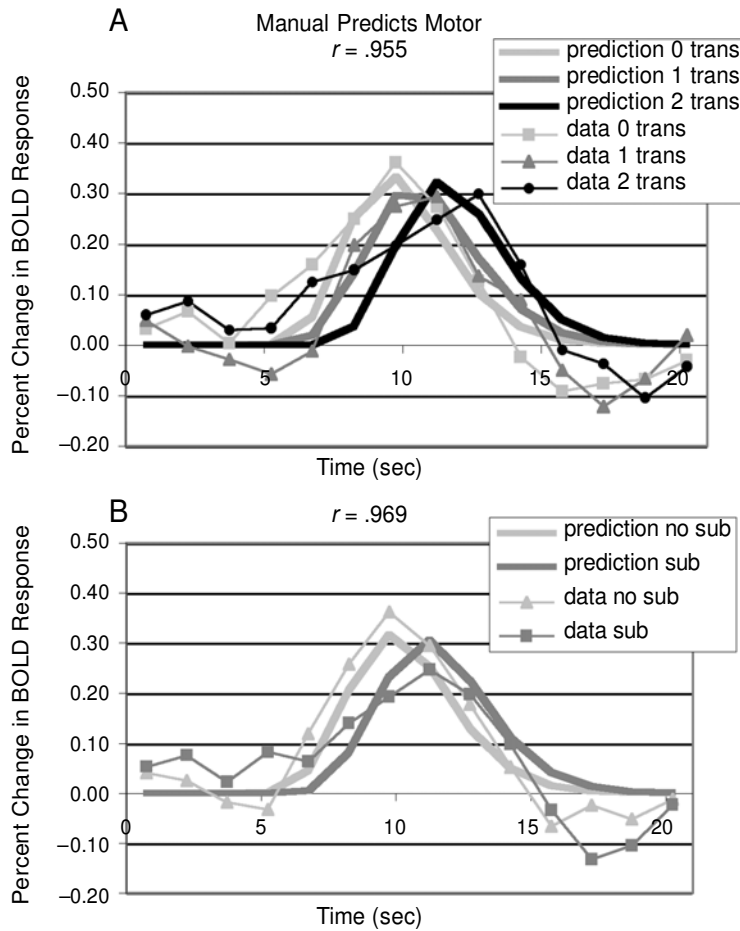
A

Manual Predicts Motor
r = .955

Legend:
- prediction 0 trans
- prediction 1 trans
- prediction 2 trans
- data 0 trans
- data 1 trans
- data 2 trans

Y-axis: Percent Change in BOLD Response (0.50, 0.40, 0.30, 0.20, 0.10, 0.00, −0.10, −0.20)
X-axis: Time (sec) (0, 5, 10, 15, 20)

B

r = .969

Legend:
- prediction no sub
- prediction sub
- data no sub
- data sub

Y-axis: Percent Change in BOLD Response (0.50, 0.40, 0.30, 0.20, 0.10, 0.00, −0.10, −0.20)
X-axis: Time (sec) (0, 5, 10, 15, 20)

Figure 14. Ability of manual buffer to predict the motor particle: (A) effects of number of transformations and (B) effects of substitution.

$p < .0001$]. As can be seen, these latency effects are consistent with the ACT–R model that we will present. A trial was scored as correct if the thumbpress occurred within 18 sec and the remaining four keys were all correct and occurred within their allotted 1.5-sec intervals. Overall accuracy was 75.1% and showed a strong negative correlation with latency ($r = -.987$). Again, our analysis of latency and fMRI was restricted to trials in which the participant was correct.

ROIs were selected according to the interaction term in a 3 conditions × 12 scans ANOVA. The 12 scans consisted of the two 1.5 scans before presentation of the equation and the 10 scans afterward (see Figure 15). To have a conservative test that dealt with nonindependence of scans, we used the Greenhouse–Geisser correction of assigning only two degrees of freedom to the numerator in the *F* statistic for the interaction term. The interaction was examined in each voxel, and the selected regions met the criteria of a minimum of six contiguous voxels, with a significant interaction at $p \leq .01$. Figure 17 and Table 7 give the eight regions that achieved this level of

significance.[7] Many of the regions overlap with those found in the first experiment. ROI 2 in this experiment is a large bilateral posterior parietal region, which includes ROIs 1 and 3 from the previous experiment. ROI 5 in this experiment is a left prefrontal particle somewhat intermediate between the similarly behaving ROIs 4 and
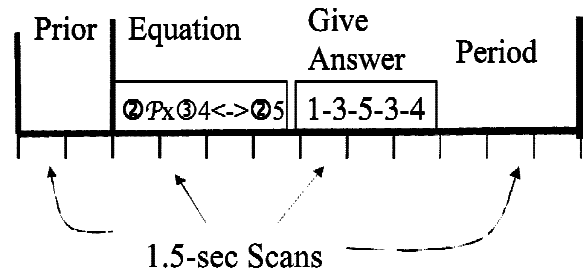
Prior | Equation | Give Answer | Period

②𝒫x③4<->②5 | 1-3-5-3-4

1.5-sec Scans

Figure 15. The 18-sec portion of an fMRI trial that was analyzed in Experiment 2. In the answer, 1 represents the thumbpress.
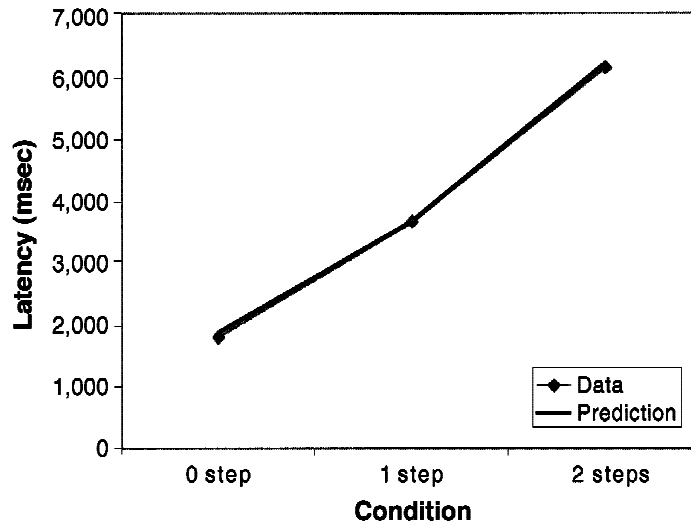
Figure 16. Mean latency in Experiment 2 as a function of the number of transformations.

5 from the previous experiment. ROIs 6 and 7 in this experiment correspond to the regions with the same numbering as that from the previous experiment. There is no region corresponding to ROI 2 (anterior cingulate) from the previous experiment. On the other hand, this experiment has ROI 1, which represents a motor area, and ROI 4, which is a polar frontal particle. There are also two small particles, ROIs 3 and 8.

Figure 18 shows the average responses in these eight ROIs as percentages of activation over the baseline defined as the average of Scans 1–3 (where the function seemed relatively flat), except for ROI 1. In the case of the motor ROI 1, the BOLD response seemed to be still coming down on Scan 1, and so we set the baseline to be defined by Scans 2–4, which seemed relatively flat. The parietal (ROIs 2 and 3), prefrontal (ROI 5), motor (ROI 1), and supramarginal (ROIs 6 and 7) regions show behavior similar to that observed in the first experiment. The polar frontal region (ROI 4) shows a large negative response, as has been observed in other studies (Gusnard & Raichle, 2001).

To provide consistency with our prior modeling effort, we will use the same ROIs as those in Experiment 1—the posterior parietal particle and the prefrontal particle (ROIs 1 and 5 from the first experiment), along with the motor particle (ROI 1 in this experiment). They are illustrated in Figure 6. Figure 19 displays the behavior of these three particles as a function of scan and condition. The figure also contains the predictions of the model that we will describe shortly. The three regions are quite distinct in their behavior. Both the parietal particle and the prefrontal particle show a response that varies in magnitude with number of transformations. However, the parietal particle shows a substantial response even in the presence of no transformations, whereas the prefrontal particle shows no response in this case. The motor particle does not show a differential magnitude of response but shows a differential delay in the response as a function of number of transformations.

Figure 20 illustrates the activity of the ACT–R modules during a solution of one of these equations. The encoding begins with the identification of $\leftrightarrow$ sign and then

Table 7
Regions of Interest, Locations of Centroid, and Significances for Experiment 2

| Region of Interest | Brodmann Area | Voxel Count | Stereotaxic Coordinates (mm) | | | F | |
			x	y	z	Maximum	Average
1. Left motor	1–4	290	−40	−24	49	16.10	9.56
2. Bilateral posterior parietal	39, 40	710	−2	−66	36	26.75	8.59
3. Left posterior parietal	40	6	−33	−49	43	6.95	6.70
4. Polar frontal	10	191	−2	55	19	10.50	7.84
5. Left prefrontal	46/9	31	−45	21	26	8.87	7.43
6. Right supramarginal gyrus	40	25	63	−26	26	9.44	7.46
7. Left supramarginal gyrus	40	28	−54	−24	19	10.55	7.69
8. Right lingual gyrus	19	11	13	−54	2	7.42	6.84
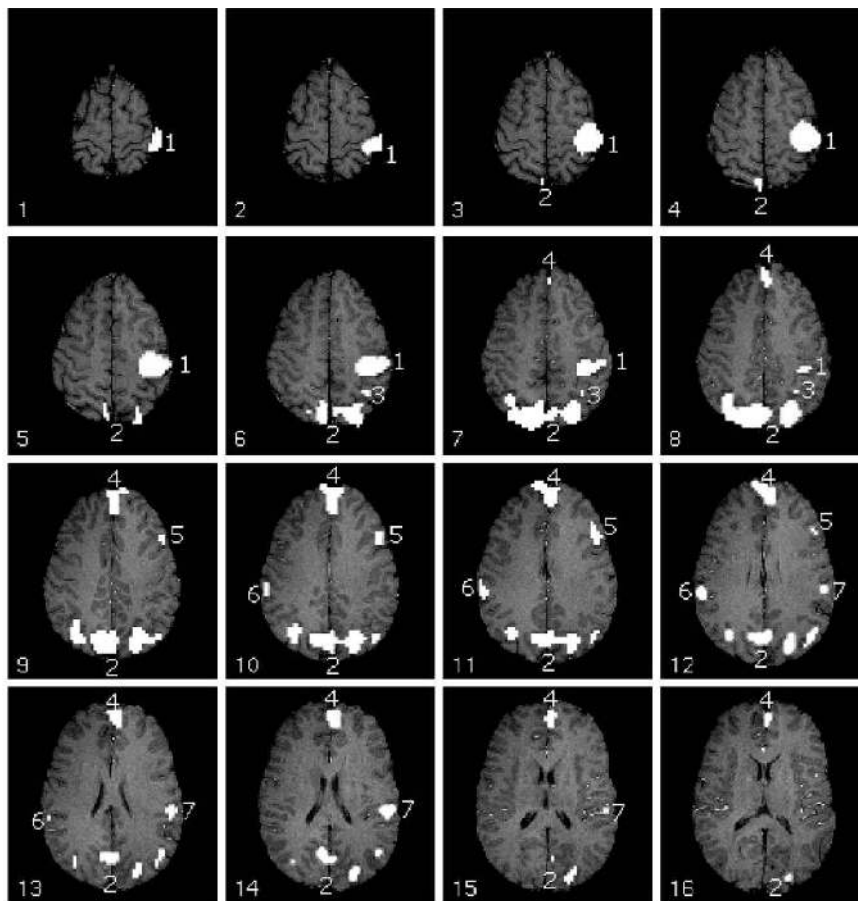
Figure 17. Activation map for the top 16 slices showing areas in Experiment 2 with a significant interaction between scan and condition. Only regions with more than six contiguous voxels and *p* < .01 are shown. See Table 6 for identification of the regions. The AC–PC line is 5 slices below Slice 16 in this figure.

the encoding of the symbols to the right of the sign. Then begins the process of encoding the elements to the left of the sign and their elimination in order to isolate the *x* . This is similar to the process, in the previous algebra experiment, of encoding the value to the right of the equal sign, followed by undoing the operations to the left of the sign in order to isolate the X. In the example in Figure 20, 6 operations are required to encode the string, and an additional 2 operations to execute the transformation. If there were no transformations there would be 5 encoding operations, which is 3 less (one less symbol on the screen and two fewer symbols to change). If there were two transformations, there would be 10 operations, because two additional symbols would have to be changed. With respect to retrievals, two pieces of information have to be retrieved to remove an operator from the *x* , and three pieces of information to move the two symbols after the *x* to the right side of the equation. In the case of an operator before the *x* , one retrieval is required to retrieve the operation to perform ("flip" in Figure 20) and the other to retrieve the identity of the terms

to apply this operation to (argument position in Figure 20). In the case of an operator and an operand after the *x* , one retrieval is required to retrieve the rule for the operand (which is copy), one to retrieve the rule for the operator (which is exchange), and one to retrieve the value it is supposed to be changed to. Thus, there are 5, 8, or 10 visual operations and 0, 2, or 5 retrieval operations. In all cases, there are the final 5 motor operations, but the time to initiate them will vary with how long the overall process takes. As in the previous experiment, the time for the encoding operations was 0.2 sec. To fit the latency date in Figure 19, we estimated a mean retrieval time of 0.65 sec (as compared with 0.6 sec in Experiment 1). The first motor action takes 0.4 sec, but because of features saved in programming subsequent fingerpresses, the remaining actions take 0.3 sec.

Table 8 reproduces the measures of proportionality between the area under the BOLD function (for parietal and prefrontal, height of Scans 4–12 above the baseline set by Scans 1–3; for motor, height of Scans 5–12 above the baseline set by Scans 2–4) and the time the buffers
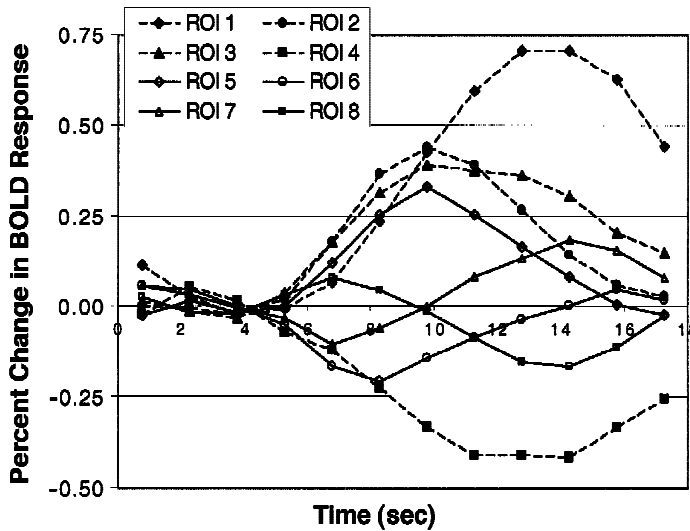
Figure 18. Average activation functions for the eight regions of interest from Experiment 2.

were active. It again confirms the association of the parietal region with the imaginal buffer, the prefrontal region with the retrieval buffer, and the motor region with the manual buffer. It is worth emphasizing that getting these strong proportionality associations is a precondition for the model-fitting enterprise. For instance, no amount of parameter estimation will ever make the retrieval fit any region other than the prefrontal region.

On the other hand, just getting these proportionality results does not guarantee that we can fit the actual BOLD functions in the various regions with the behavior of the corresponding buffers. Thus, successfully fitting the BOLD functions is a more stringent test of the correspondence. To determine these fits required estimation of the three parameters of the BOLD function for each region. These are reproduced in Table 5, to facilitate comparison with Experiment 1. The parameters for the imaginal and retrieval buffers are quite similar across the two experiments. The manual buffer parameters are quite different, probably reflecting the poor signal-to-noise ratio in Experiment 1 and, hence, unreliable parameter estimates.

The degrees of freedom are the 108 observations (3 regions $\times$ 3 conditions $\times$ 12 scans) minus the 9 parameters, or 99. The chi-square deviation was 135.50, which is significant and once again indicates that our fit is only approximate. Nonetheless, as can be seen from Figure 19, the model does a good job in accounting for the behavior of the three regions. In this experiment with the five finger movements, the behavior in the motor region provided a strong signal that was well fit by the model. As was predicted, the peak of the BOLD function shifts with condition. The fit to the prefrontal particle may be again suffering from the failure of the current BOLD function to predict an undershoot at the end of the BOLD response. The prediction for the prefrontal particle in the zero-transformation condi-

tion is particularly dramatic—a flat function, because there are no retrievals. Although the actual data for the prefrontal region may show the slightest of rises and undershoots in this condition, they provide a close approximation to this strong parameter-free prediction.

GENERAL DISCUSSION

First, we would like to begin with some discussion of the approximations in our mathematical treatment. As has already been noted, we ignore the potential undershoot as the function goes back to baseline. In addition, we have ignored the variability in the timing of responses between and within subjects, and the model assumes a single mean time for the processing in each condition. The consequence of this approximation perhaps shows up most clearly in Figure 19C, where the longer and more variable two-transformation condition resulted in a lower and wider BOLD response. We think that these approximations are more than justified by the greater simplicity and interpretability of the resulting model. We do not think that they at all compromise the basic conclusions.

A more fundamental issue has to do with the assumption that the BOLD response increases linearly with the length of an event and is additive across multiple events. Although there is evidence for this as an approximate char-

Table 8
Measures of Proportionality Between Buffer Activity and Area Under the BOLD Function in Experiment 2

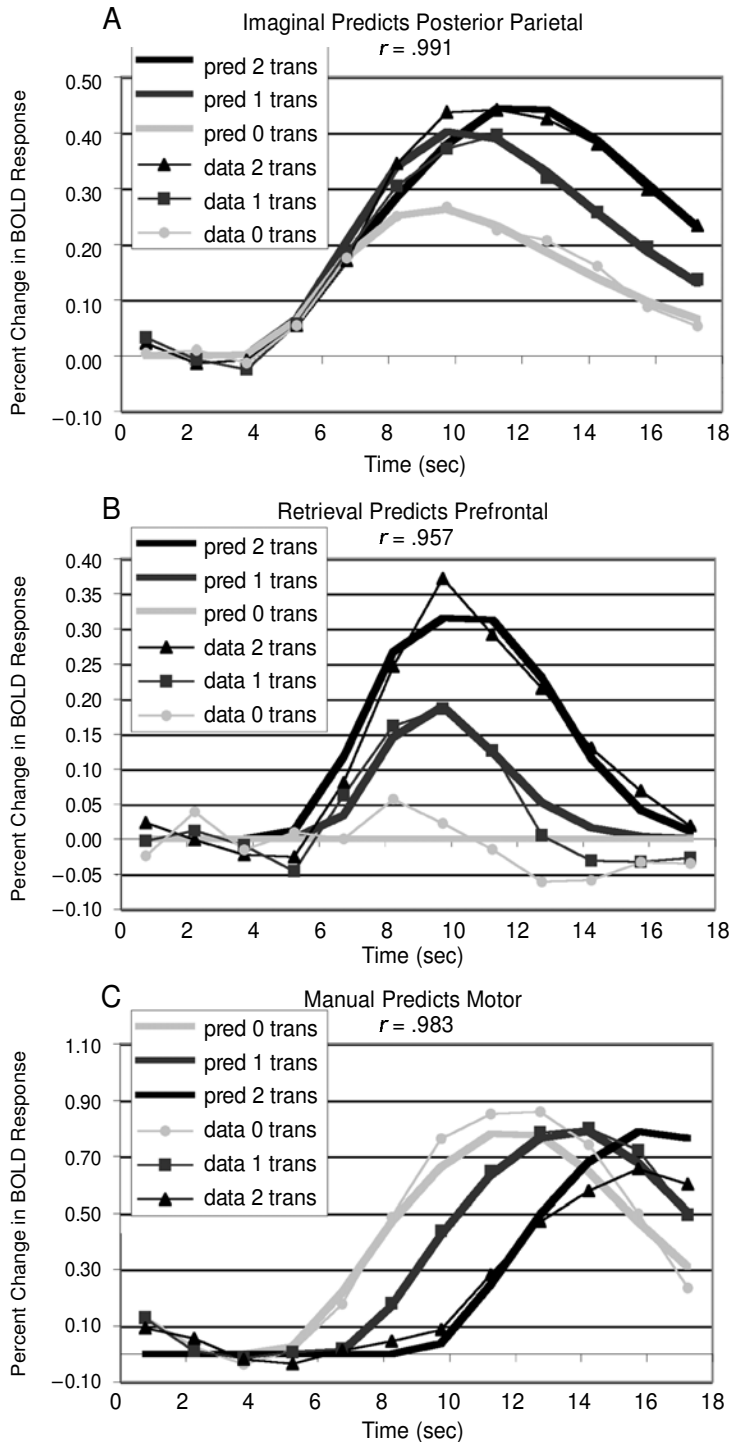| Buffer	Parietal	Prefrontal	Motor
Imaginal	.999	.678	.803
Retrieval	.782	.984	.361
Manual	.942	.445	.958

Figure 19. BOLD response in Experiment 2 as a function of scan for 0, 1, and 2 transformations: (A) posterior parietal particle, (B) prefrontal particle, and (C) motor particles.

acterization in some situations (e.g., Boyton et al., 1996; Dale & Buckner, 1997), it does not seem to be universally the case (e.g., Glover, 1999), with there being evidence for sublinear growth with duration and subadditivity across events. Potentially, this could seriously compromise the logic of this and related research in a way that we could not recover from without a basis for characterizing the nonlinearities and nonadditivities. It remains an open
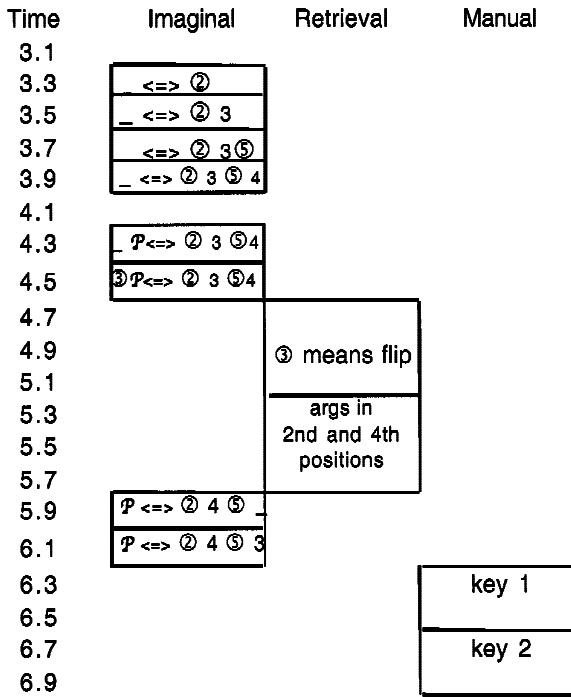
Figure 20. The approximate time line for the buffer activity in the ACT–R model for Experiment 2.

issue just how serious a matter this is, but in our mind, it is the major question about the modeling methodology in this article.

As an empirical summary, this research is largely consistent with existing associations, in the literature, of the parietal cortex with visual and imaginal processing, the prefrontal cortex with retrieval, and the region of the motor and somatosensory cortex that represents the right hand with the manual buffer. Each of these associations deserves a little comment. First, although there was bilateral activation of the parietal cortex, it was stronger in the left, consistent with other research on arithmetic and imagery processing in language. This is perhaps consistent with the semantic and somewhat abstract nature of the task. Perhaps the reason that the activation was more bilateral in the second experiment is that we had removed most of the semantic associations and had made it a more purely visual task.

Second, our prefrontal retrieval focus was found in left BA 45/46. According to the HERA model, the left prefrontal cortex has been associated with semantic retrieval. However, much of what the participants in our experiment were retrieving was not classically semantic information. The algebraic knowledge and arithmetic knowledge in the first experiment would seem classically semantic, but we also found an effect of retrieval of just-memorized constant values in Experiment 1 and of algebraic transformations just learned in Experiment 2. Although our retrievals were not semantic in the sense of having been long-learned, they were semantic in the sense of being decontextualized knowledge. So perhaps our results lend some definition to the association of the left prefrontal cortex with *semantic* retrieval. Also, our region was anterior to BA 44, which seems to have mostly been found in previous studies of semantic retrieval. We did find a similar pattern of activation in superior BA 44 (as indicated by the correlation in Table 3 between ROIs 4 and 5). However, we focused on BA 45/46, in part because it was more strongly related to number of transformations, showing no rise at all when there were no retrievals required. Interestingly, episodic retrieval seems to activate right BA 46 more often than right BA 44 (Cabeza & Nyberg, 2000). However, we should note that there are other interpretations of the left–right asymmetry besides the HERA model. For instance, it has been argued that the right hemisphere is more related to the retrieval mode, whereas the left is associated with past-retrieval products (e.g., Lepage, Ghaffar, Nyberg, & Tulving, 2000). This would be consistent with ACT–R's retrieval buffer that holds the products of retrieval.

Third, we should comment on the association of our manual buffer with activation in the somatosensory area corresponding to the right hand, as well as with the motor area. In fact, the motor ROI is similar to the region identified by Roland, Larsen, Lassen, and Skinhoj (1980) when a finger is pressed. In the descending motor pathway (Pyramidal tract) for voluntary movement, fibers come from both the precentral (BAs 4, 6) and the postcentral (BAs 3a, 5; Kolb & Wilshaw, 1990) areas.

This article is built around a tentative mapping from ACT–R buffers to the BOLD response. Undoubtedly, this mapping will have to be revised with further evidence. However, we think the most important contribution of this article is the conception it offers of how the detailed processing of an information-processing theory such as ACT–R can make precise predictions about the BOLD response. We would hope that this conception would survive any revisions in ACT–R and its mapping to brain function. Indeed, we would hope that this same conception can be incorporated by other information-processing theories.

The basic idea is that the BOLD response reflects the duration for which various cognitive modules are active. The typical additive factors information-processing methodology has studied how manipulations of various cognitive components affect a single aggregate behavioral measure, such as total time. If we can assign these different components to different regions, we essentially have a separate dependent measure to track each component. Therefore, this methodology promises to offer strong guidance in the development of an information-processing theory.

Finally, we want to comment on the surprising match of fMRI methodology to the study of complex tasks. A problem with fMRI is its poor temporal resolution. However, as is particularly apparent in the behavior of our manual buffer (Figure 19C), the typical effect size in a complex mental task is such that one can still make temporal discriminations in fMRI data. One might have thought that the outcome of such a complex task would

be purely uninterpretable. However, with the guidance of a strong information-processing model and well-trained participants, one can not only interpret, but also predict the BOLD response in various regions of the brain.

The principal function of this article has been to show how to relate an information-processing model such as ACT–R to fMRI data. That connection is a two-way street. Going from modeling to fMRI data allows one to interpret the significance of the data in terms of precise information-processing operations, rather than in terms of relatively diffuse concepts. For instance, it makes clear how one can conceive of differences in the BOLD function as reflecting differences in duration of cognitive components, rather than differences in intensity of cognitive components, as is the more common conception. This is important because standard information-processing theories have more often been developed in terms of the effects of manipulations on the durations of stages.

Going from the data to modeling, it means that we can use such experiments to test predictions of the theory. For instance, the theory would predict that, with practice, the retrieval steps in charts like Figures 8 and 20 should shorten, whereas the imaginal and retrieval steps should stay relatively constant. Therefore, the theory predicts that activation should decrease in the prefrontal region but that such a decrease would not occur in our parietal or motor regions. Thus, we can perform tests on components of our theory in a way that was not possible when we simply had total latency to work with. It is certainly conceivable that the greater level of identifiability will force revisions in the theory that would not happen otherwise.

REFERENCES

Amos, A. (2000). A computational model of information processing in the frontal cortex and basal ganglia. *Journal of Cognitive Neuroscience, 12*, 505-519.

Anderson, J. R., & Lebiere, C. (1998). *The atomic components of thought.* Mahwah, NJ: Erlbaum.

Anderson, J. R., Reder, L. M., & Lebiere, C. (1996). Working memory: Activation limitations on retrieval. *Cognitive Psychology, 30*, 221-256.

Ashby, F. G., & Waldron, E. M. (2000). The neuropsychological bases of category learning. *Current Directions in Psychological Science, 9*, 10-14.

Awtry, T., & Kirshner, D. (1994). Visual salience in algebraic transformations. In *Proceedings of the Sixteenth Annual Meeting of the International Group for the Psychology of Mathematics Education, North American Chapter* (PME-NA XIII). Louisiana State University.

Berman, K. F., Ostrem, J. L., Randolph, C., Gold, J., Goldberg, T. E., Coppola, R., Carson, R. E., Herscovitch, P., & Weinberger, D. R. (1995). Physiological activation of a cortical network during performance of the Wisconsin card sorting test: A positron emission tomography study. *Neuropsychologia, 33*, 1027-1046.

Blessing, S. B. (1996). *The use of prior knowledge in learning from examples.* Unpublished doctoral dissertation, Carnegie Mellon University, Pittsburgh.

Blessing, S. B., & Anderson, J. R. (1996). How people learn to skip steps. *Journal of Experimental Psychology: Learning, Memory, & Cognition, 22*, 576-598.

Boyton, G. M., Engel, S. A., Glover, G. H., & Heeger, D. J. (1996). Linear systems analysis of functional magnetic resonance imaging in human V1. *Journal of Neuroscience, 16*, 4207-4221.

Byrne, M. D., & Anderson, J. R. (1998). Perception and action. In J. R. Anderson & C. Lebiere (Eds.), *The atomic components of thought* (pp. 167-200). Mahwah, NJ: Erlbaum.

Cabeza, R., & Nyberg, L. (2000). Imaging cognition II: An empirical review of 275 PET and fMRI studies. *Journal of Cognitive Neuroscience, 12*, 1-47.

Cohen, M. S. (1997). Parametric analysis of fMRI data using linear systems methods. *NeuroImage, 6*, 93-103.

Dale, A. M., & Buckner, R. L. (1997). Selective averaging of rapidly presented individual trials using fMRI. *Human Brain Mapping, 5*, 329-340.

Dehaene, S., Spelke, E., Pinel, P., Stanescu, R., & Tsivkin, S. (1999). Sources of mathematical thinking: Behavior and brain-imaging evidence. *Science, 284*, 970-974.

Forman, S. D., Cohen, J. D., Fitzgerald, M., Eddy, W. F., Mintun, M. A., & Noll, D. C. (1995). Improved assessment of significant activation in functional magnetic resonance imaging (fMRI): Use of a cluster-size threshold. *Magnetic Resonance in Medicine, 33*, 636-647.

Frank, M. J., Loughry, B., & O'Reilly, R. C. (2000). *Interactions between frontal cortex and basal ganglia in working memory: A computational model* (Tech. Rep. 00-01). Boulder: University of Colorado, Institute of Cognitive Science.

Glover, G. H. (1999). Deconvolution of impulse response in event-related BOLD fMRI. *NeuroImage, 9*, 416-429.

Goldberg, T. E., Berman, K. F., Fleming, K., Ostrem, J., Van Horn, J. D., Esposito, G., Mattay, V. S., Gold, J. M., & Weinberger, D. R. (1998). Uncoupling cognitive workload and prefrontal cortical physiology: A PET rCBF study. *NeuroImage, 7*, 296-303.

Grafman, J., & Rickard, T. C. (1996). Acalculia. In T. E. Fineberg & M. J. Farah (Eds.), *Behavioral neurology and neuropsychology* (pp. 219-225). New York: McGraw-Hill.

Gruber, O., Indefrey, P., Steinmetz, H., & Kleinschmidt, A. (2000). Dissociating neural correlates of cognitive components in mental calculation. *Cerebral Cortex, 11*, 350-359.

Gusnard, D. A., & Raichle, M. E. (2001). Searching for a baseline: Functional imaging and the resting human brain. *Nature Reviews: Neuroscience, 2*, 685-694.

Hikosaka, O., Nakahara, H., Rand, M. K., Sakai, K., Lu, Z., Nakamura, K., Miyachi, S., & Doya, K. (1999). Parallel neural networks for learning sequential procedures. *Trends in Neurosciences, 22*, 464-471.

Houk, J. C., & Wise, S. P. (1995). Distributed modular architectures linking basal ganglia, cerebellum, and cerebral cortex: Their role in planning and controlling action. *Cerebral Cortex, 2*, 95-110.

Huettel, S. A., & McCarthy, G. (2000). Evidence for refractory period in the hemodynamic response to visual stimuli as measured by MRI. *NeuroImage, 11*, 547-553.

Jackson, M., & Warrington, E. K. (1986). Arithmetic skills in patients with unilateral cerebral lesions. *Cortex, 22*, 610-620.

Just, M. A., Carpenter, P. A., & Varma, S. (1999). Computational modeling of high-level cognition and brain function. *Human Brain Mapping, 8*, 128-136.

Kastrup, A., Krüger, G., Glover, G. H., Neumann-Haefelin, T., & Moseley, M. E. (1999). Regional variability of cerebral blood oxygenation response to hypercapnia. *NeuroImage, 10*, 675-681.

Kirshner, D. (1989). The visual syntax of algebra. *Journal for Research in Mathematics Education, 20*, 274-287.

Kolb, B., & Wilshaw, I. (1990). *Fundamentals of human neuropsychology* (3rd ed.). New York: Freeman.

Lepage, M., Ghaffar, O., Nyberg, L., & Tulving, E. (2000). Prefrontal cortex and episodic memory retrieval mode. *Proceedings of the National Academy of Sciences, 97*, 506-511.

MacDonald, A. W., III, Cohen, J. D., Stenger, V. A., & Carter, C. S. (2000). Dissociating the role of the dorsolateral prefrontal and anterior cingulate cortex in cognitive control. *Science, 288*, 1835-1838.

Menon, V., Rivera, S. M., White, C. D., Glover, G. H., & Reiss, A. L. (2000). Dissociating prefrontal and parietal cortex activation during arithmetic processing. *NeuroImage, 12*, 357-365.

Meyer, D. E., & Kieras, D. E. (1997a). A computational theory of executive cognitive processes and multiple-task performance: Pt. 1. Basic mechanisms. *Psychological Review, 104*, 2-65.

Meyer, D. E., & Kieras, D. E. (1997b). A computational theory of ex-

ecutive cognitive processes and multiple-task performance: Pt. 2. Accounts of psychological refractory-period phenomena. *Psychological Review*, **104**, 749-791.

NYBERG, L., CABEZA, R., & TULVING, E. (1996). PET studies of encoding and retrieval: The HERA model. *Psychonomic Bulletin & Review*, **3**, 135-148.

PEW, R. W., & MAVOR, A. S. (1998). *Modeling human and organizational behavior: Application to military simulations*. Washington, DC: National Academy Press.

REICHLE, E. D., CARPENTER, P. A., & JUST, M. A. (2000). The neural basis of strategy and skill in sentence–picture verification. *Cognitive Psychology*, **40**, 261-295.

RICKARD, T. C., ROMERO, S. G., BASSO, G., WHARTON, C. M., FLITMAN, S., & GRAFMAN, J. (2000). The calculating brain: An fMRI study. *Neuropsychologia*, **38**, 325-335.

ROLAND, P. E., LARSEN, B., LASSEN, N. A., & SKINHOJ, E. (1980). Supplementary motor area and other cortical areas in organization of voluntary movements in man. *Journal of Neurophysiology*, **43**, 118-136.

ROSSELLI, M., & ARDILA, A. (1989). Calculation deficits in patients with right and left hemisphere damage. *Neuropsychologia*, **27**, 607-617.

SAINT-CYR, J. A., TAYLOR, A. E., & LANG, A. E. (1988). Procedural learning and neostriatal dysfunction in man. *Brain*, **111**, 941-959.

SOHN, M.-H., URSU, S., ANDERSON, J. R., STENGER, V. A., & CARTER, C. S. (2000). The role of prefrontal cortex and posterior parietal cortex in task switching. *Proceedings of the National Academy of Science*, **97**, 13448-13453.

TULVING, E., KAPUR, S., CRAIK, F. I. M., MOSCOVITCH, M., & HOULE, S. (1994). Hemispheric encoding/retrieval asymmetry in episodic memory: Positron emission tomography findings. *Proceedings of the National Academy of Sciences*, **91**, 2016-2020.

WISE, S. P., MURRAY, E. A., & GERFEN, C. R. (1996). The frontal cortex–basal ganglia system in primates. *Critical Reviews in Neurobiology*, **10**, 317-356.

WOODS, R. P., GRAFTON, S. T., HOLMES, C. J., CHERRY, S. R., & MAZZIOTTA, J. C. (1998). Automated image registration: I. General methods and intrasubject, intramodality validation. *Journal of Computer Assisted Tomography*, **22**, 139-152.

ZAGO, L., PESENTI, M., MELLET, E., CRIVELLO, F., MAZOYER, B., & TZOURIO-MAZOYER, N. (2001). Neural correlates of simple and complex mental calculation. *NeuroImage*, **13**, 314-327.

NOTES

1. The earlier Anderson, Reder, & Lebiere (1996) studies were also concerned with an interaction between the size of the load and the physical complexity of the equation. This is an issue that we will not be pursuing here, and indeed, we strive to keep the physical complexity of the equation constant.

2. See http://kraepelin.wpic.pitt.edu/nis/index.html.

3. Basically, we are convolving the BOLD function with the function $i(x)$, giving the activity of that buffer.

4. Thus, it does establish that only the buffer associated with the region could predict the BOLD function in that region and that the other buffers could not.

5. The chi-square is a measure of the amount the predictions deviate from the noise, and this measure indicates that they deviate less than 50% greater than expected. By way of contrast, if we try to fit the manual buffer to the prefrontal region, the retrieval buffer to the parietal region, and the imaginal buffer to the motor region, the chi-square is 1,079.66, which is more than four times greater than expected.

6. A model in an earlier version of ACT–R for a learning version of this task is to be found in Blessing (1996).

7. ROI 8 is a small particle occurring in Slices 18–20, not shown in Figure 17.